Title: Renal tubular arginase-2 participates in the formation of the corticomedullary urea gradient and attenuates kidney damage in ischemia-reperfusion injury in mice.

Authors: Ansermet C., Centeno G., Lagarrigue S., Nikolaeva S., Yoshihara H.A., Pradervand S., Barras J.L., Dattner N., Rotman S., Amati F., Firsov D.

Journal: Acta Physiologica

Year: 2020

DOI: https://doi.org/10.1111/apha.13457

Renal tubular Arginase-2 participates in the formation of the corticomedullary urea gradient and attenuates kidney damage in ischemia-reperfusion injury in mice.

Camille Ansermet[1#], Gabriel Centeno[1#], Sylviane Lagarrigue[2#], Svetlana Nikolaeva[1,3], Hikari AI Yoshihara[4], Sylvain Pradervand[5], Jean-Luc Barras[6], Nicolas Dattner[6], Samuel Rotman[6], Francesca Amati[2], Dmitri Firsov[1]

[1] - Department of Pharmacology and Toxicology, University of Lausanne, Switzerland
[2] - Department of Physiology & Institute of Sport Sciences, University of Lausanne, Switzerland
[3] - Institute of Evolutionary Physiology and Biochemistry, St-Petersburg, Russia
[4] - Institute of Physics, Ecole Polytechnique Fédérale de Lausanne, Switzerland
[5] - Genomic Technologies Facility, University of Lausanne, Switzerland
[6] - Service of Clinical Pathology, Lausanne University Hospital, Institute of Pathology, Switzerland

[#] - these authors contributed equally to this work

* - to whom correspondence should be addressed:
Dmitri Firsov, Department of Pharmacology and Toxicology, University of Lausanne, 27 rue du Bugnon, 1005 Lausanne, Switzerland. Phone: ++ 41-216925406 Fax: ++ 41-216925355
e-mail: dmitri.firsov@unil.ch

short title: role of Arginase-2 in the renal tubule

ABSTRACT

RESULTS

Basic characteristics of Arg2$^{lox/lox}$/Pax8-rtTA/LC1 (cKO) mice. Conditional inactivation of the *Arg2* gene in the renal tubule was induced by 2-week treatment with doxycycline (DOX, 2 mg/ml in drinking water) of 8-week old *Arg2*$^{lox/lox}$/Pax8-rtTA/LC1 male mice (hereafter referred to as conditional knockout mice or cKO mice, see Supplementary Methods). In parallel the same DOX treatment was provided to their littermate controls (*Arg2*$^{lox/lox}$ mice, hereafter referred to as control mice). To avoid potential side effects related to DOX toxicity all experiments were performed 1 month after the end of DOX treatment. As shown in Figure 1, Arg2 mRNA (Figure 1A) and protein (Figure 1B) expression, as well as arginase activity (Figure 1C) were significantly reduced in kidneys of cKO mice. Because previous studies have reported that Pax8-driven LC1-Cre recombinase is expressed in a subset of periportal hepatocytes[21,22], we examined Arg2 expression in the liver of control and cKO mice. As shown in Figure 1D, there was no difference in hepatic Arg2 expression between control and cKO mice. These experiments also demonstrated that expression levels of Arg2 in the liver of both genotypes were significantly lower than in the kidney (Figure 1A versus Figure 1D). The cKO mice were apparently normal, their body weight was not different from control mice (Supplementary Table 1) but their kidney weight/body weight ratio was significantly lower (Figure 1E). Measured plasma and urine parameters were not different between control and cKO mice (Supplementary Table 1). Because, Huang et al. have shown that the urine concentration ability is decreased in *Arg2*-null mice via a mechanism that negatively controls the aquaporin-2 (AQP2) water channel expression[20], we subjected the control and cKO mice to water deprivation for 12 hours. As shown in Supplementary Table 1, the water deprivation test did not reveal significant difference in urine volume and osmolality between control and cKO mice. Expression levels of aquaporin-2 (Aqp2), aquaporin-3 (Aqp3), aquaporin-4 (Aqp4) and

V2 type vasopressin receptor (Avpr2) mRNAs were not different between control and cKO mice that received water *ad libitum*, but were lower in kidneys of water-deprived cKO mice as compared to water-deprived control mice (Supplementary Figure 1A). However, AQP2 protein expression was similar under water deprivation in both genotypes (Supplementary Figure 1B). These results differ significantly from those published for *Arg2*-null mice[20].

Role of ARG2 in the early phase of renal injury triggered by IR: 24-hour reperfusion. The role of ARG2 in the early events in IR-induced renal injury was studied 24 hours after unilateral IR injury (UIRI) or sham surgery. As shown in Figure 2A, Arg2 mRNA expression was significantly increased in the left ischemic kidney of control mice as compared to the contralateral (right) kidney and to kidneys from sham-operated animals. Arg2 expression was also increased in the left ischemic kidney from cKO mice (Figure 2B). However, quantitatively, Arg2 levels in kidneys of cKO mice remained negligible compared to those of control mice. Immunohistochemical analysis revealed dramatically increased ARG2 expression in the medulla of the left ischemic kidney in control mice, as compared to the right kidney (Figure 2C). Histological scoring of Periodic Acid-Schiff (PAS)-stained kidney sections from control and cKO mice (Figures 3A and 3B, respectively) demonstrated significantly greater tubular damage in the medulla of the left ischemic kidney from cKO mice (Figure 3C). TUNEL assay showed a diffuse staining of damaged tubules in kidneys of UIRI-subjected control and cKO mice (Figures 3D and 3E, respectively, and Supplementary Figure 2), characteristic of necrotic cell death. Quantitation of TUNEL staining revealed a similar trend towards higher cellular damage in UIRI-subjected cKO mice ($p=0.058$, Figure 3F). Expression levels of most tested early tissue AKI biomarkers (Kim-1, Il-6 and Tnf-α) were increased in left ischemic kidneys of both genotypes but not different between control and cKO mice (Supplementary Figure 3).

However, expression of fibrinogen gamma chain (Fgg) was significantly higher in left ischemic kidneys of cKO mice, suggesting enhanced wound repair[23,24] (Supplementary Figure 3).

Analysis of urine samples collected in metabolic cages over 24 hours following UIRI revealed significantly greater functional impairments in cKO mice. As shown in Table 1, cKO mice exhibited albuminuria, kaliuria, calciuria, magnesuria, polyuria, increased urinary urea excretion and generalized aminoaciduria (Supplementary Figure 4). Analysis of blood collected 24 hours after sham or UIRI surgery showed no significant difference in plasma creatinine levels (Table 1). Urea concentration was slightly but significantly higher in UIRI-subjected control mice, thus correlating with increased ARG2 expression (Table 1 and, see below).

Sham-operated mice were also used to test the possible role of renal ARG2 in the formation of corticomedullary urea gradient. To this aim, we measured urea content in the cortex, outer medulla and inner medulla of right and left kidneys from sham-operated control and cKO mice. As shown in Figure 4A, urea content was significantly lower in the outer and inner medulla of both right and left kidneys from sham-operated cKO mice as compared to control mice (*n.b.* – *p*-value for comparison of urea content in the outer medulla of the right kidney of sham-operated control and cKO mice = 0.054). Thus, these data support the idea that the S3-located ARG2 participates to the formation of urea concentration gradient along the corticomedullary axis. The lower medullary urea content in cKO mice was associated with statistically significant but quantitatively modest decrease in the total osmolyte content of the outer medulla in both right and left kidneys from sham-operated cKO mice as compared to control mice (Figure 4B; *n.b.* – the total osmolyte content in the inner medulla could not be measured due to the small sample size).

UIRI caused a dramatic decrease in urea content in left ischemic kidneys from both genotypes (Figure 4C). However, urea and the total osmolyte contents in the outer and inner medulla were not different in left kidneys of UIRI-subjected control and cKO mice (Figure 4D).

These results suggest that polyuria observed in cKO mice subjected to UIRI (Table 1) is caused by osmotic diuresis and/or results from a dysfunction in the tubular mechanism of water reabsorption rather than from a difference in corticomedullary osmotic gradients in kidneys of control and cKO mice.

Role of ARG2 in long-term consequences of UIRI: 14 days reperfusion. It has been shown that in the model of UIRI with an intact contralateral kidney the ischemic kidney exhibit long-term progression towards chronic kidney disease (CKD)[25,26]. Fourteen days after UIRI the cKO mice had significantly lower body weight compared to UIRI-subjected controls (Figure 5A). UIRI induced compensatory hypertrophy of the contralateral (right) kidney in both control and cKO mice (Figure 5B). However, this effect was significantly greater in cKO mice, thus indirectly suggesting stronger functional damage in the left ischemic kidney. ARG2 expression remained induced in the medulla of the left ischemic kidney of control mice as shown by Western blot analysis (Supplementary Figure 5) and immunohistochemistry (Figures 5C). As shown in Figure 5D, in the left ischemic kidney of control mice there was a strong positive correlation between Arg2 mRNA expression and expression levels of several markers of interstitial fibrosis (Vim, Fn1, Col3a1 and Col1a1). However, expression levels of these fibrosis markers and fibrosis score assessed by Masson's trichrome staining were not different between the two genotypes (Supplementary Figure 6A and 6B, respectively).

Analysis of urine samples showed that UIRI-subjected mice of both genotypes did not develop proteinuria and did not display major differences in urine volume and solute excretion rates (Supplementary Table 3). As shown is Supplementary Table 3, there was no difference in inulin clearance between UIRI-subjected cKO and control mice. Analysis of plasma revealed that UIRI-subjected cKO mice exhibit hypernatremia and significantly increased levels of

symmetric dimethylarginine (SDMA) and asymmetric dimethylarginine (ADMA), two early markers of kidney disease progression (Figure 5E and Supplementary Table 4)[27,28].

Compared to UIRI-subjected cKO mice, UIRI-subjected control mice had both higher plasma urea levels and lower arginine levels (Supplementary Table 3). These findings together with results showing no difference in inulin clearance between mice of the two genotypes (see above) suggest that higher plasma urea levels in control mice may result from increased ARG2 activity in the left ischemic kidney. Because ornithine generated through arginase activity can be further metabolized to polyamines (putrescine, spermidine and spermine) and proline or, used for energy production by replenishing TCA cycle intermediates[11,12], we examined kidney tissue levels of these compounds. As shown is Supplementary Figure 7, kidney tissue putrescine and spermine contents were significantly decreased in left ischemic kidneys of both genotypes. However, there was no difference in tissue levels of putrescine, spermidine, spermine and proline in left ischemic kidneys of control and cKO mice. These results prompted us to investigate possible alterations in kidney energy metabolism induced by UIRI. First, we evaluated the effect of UIRI on mitochondrial DNA content. As shown is Supplementary Figure 8, the ratio between the DNA levels of mitochondrial gene NADH dehydrogenase (mt-ND1) and nuclear cyclophilin A gene (Ppia) was markedly reduced in ischemic kidneys, most probably reflecting fibrosis. However, this reduction was similar in both genotypes. By using Seahorse analysis, the degree of coupling between the electron transport chain (ETC) and the oxidative phosphorylation machinery (OXPHOS) was examined on mitochondria isolated from kidneys of control and cKO mice (two way repeated measures ANOVA (Genotype X Left vs Right kidney)). These results demonstrated that ischemia affected mitochondrial respiration in kidneys of both, control and cKO mice (Figures 6A, 6B, 6C, 6D, 6E and Supplementary Statistical Table for Figures 1 to 6). However, a significant interaction effect in state III

respiration suggested a greater impairment in the OXPHOS machinery in the ischemic kidney of cKO mice (interaction effect p=0.015, Figure 6C).

DISCUSSION

Arginase-2 is an extensively studied enzyme involved in a wide variety of biological processes and pathophysiological conditions. Historically, arginase was among the first enzymes that were (partially) purified and biochemically characterized in the kidney[29,30]. Since then, several strategies have been developed to study the role of this enzyme in the kidney, mainly based on the use of mice with whole-body inactivation of the *Arg2* gene (*Arg2*-null mice) or, on the pharmacological inhibition of arginase activity. Here, we addressed this issue in a new mouse model in which *Arg2* was deleted specifically in the renal tubule. This new model allowed us to directly test the hypothesis raised in several studies[9-11,19] that urea formed by ARG2 might contribute to the formation of the corticomedullary urea and osmolality gradients. The present study supports this hypothesis, thereby providing new insight into the mechanism of urine formation. Our results, however, differ from those of Huang and colleagues who found in *Arg2*-null mice that ARG2 negatively regulates AQP2 expression and water reabsorption in the kidney. In our model, Aqp2 mRNA expression was reduced in kidney of cKO mice subjected to water deprivation and, AQP2 protein expression and urine conservation ability remained unchanged. We hypothesize that this discrepancy may be due to activity of ARG2 in extra-renal tissues.

Under normal conditions, no changes in plasma levels of L-arginine and urea were observed in cKO mice, suggesting that ARG2 in the kidney accounts for only a small fraction of L-arginine ureahydrolase activity in the body. However, 24 hours after UIRI plasma urea levels were significantly increased in control mice without concomitant elevation in plasma creatinine levels. Fourteen days after UIRI, higher plasma urea levels in control mice were inversely correlated with lower arginine concentration compared to cKO mice, with no difference observed in plasma creatinine levels between the two genotypes. These results suggest that UIRI-induced upregulation of ARG2 activity in the injured kidney leads to a

dramatic increase in plasma urea levels (~80% in the present study) that are not due to changes in GFR. Interestingly, similar findings have been recently described by Nikoaleva et al. in another model of renal stress, i.e. in the kidney lacking the circadian clock activity[21]. The authors demonstrated that mice devoid of the circadian clock specifically in the renal tubule exhibited a significant increase in ARG2 activity in the kidney, which reached ~25% of arginase activity in the liver. In parallel these mice showed a ~20% increase in plasma urea levels but no difference in GFR. These results may have important clinical implications because plasma urea concentration is one of the most commonly used endogenous markers of glomerular filtration. Our study demonstrates that ARG2, which is upregulated in virtually all kidney stress conditions tested so far, can significantly influence plasma urea levels, and that these changes may not reflect changes in GFR. A challenging task for future studies is to elucidate the mechanism(s) regulating Arg2 transcription. Since (i) the S3 segment of the proximal tubule is located in the renal medulla, a low oxygen environment and, (ii) the medullary oxygen tension further decreases in many types of AKI or CKD previously noted, it is plausible to hypothesize that the primary factor inducing Arg2 levels is hypoxia. However, renal Arg2 expression is also increased upon furosemide treatment (CA, GC and DF, unpublished results), a condition that increases medullary oxygen tension[31]. This suggests that a complex multifactorial mechanism is involved in Arg2 regulation.

Twenty-four hours after UIRI both histological and functional outcomes were significantly worse in cKO mice. The cKO mice exhibited significantly greater tubular damage in the ischemic kidney as compared to the ischemic kidney from control mice. Surprisingly, however, among tested mRNA markers of early injury[24] (Kim-1, Il-6, Tnf-α and Fgg), only Fgg mRNA expression was significantly higher in the ischemic kidney of cKO mice. This can be explained by the relatively poor correlation between the degree of AKI severity and expression levels of these mRNA markers, at least in the UIRI model[25]. Urine analysis revealed

that cKO mice developed polyuria, albuminuria, aminoaciduria, kaliuria, calciuria, phosphaturia and magnesuria, a phenotype reminiscent of Fanconi syndrome, or generalized dysfunction of the proximal tubule. Fanconi syndrome is a complex renal disease characterized by impaired capacity of the proximal tubule to reabsorb and/or secrete water and solutes. Importantly, while there are many different causes of Fanconi syndrome, they all give rise to a similar phenotype (see above). Thus, it has been proposed that impaired energy production could be a common mechanism responsible for abnormal tubular transport[32]. Accordingly, in addition to extensive tubular loss, altered metabolism in the proximal tubule may explain the Fanconi syndrome phenotype in the early phase of UIRI in cKO mice.

Two weeks after UIRI, the cKO mice had lower body weight but the overall renal function was not different between the two genotypes. However, significantly greater adaptive growth of the contralateral (right) kidney in cKO mice suggested more severe functional damage in the ischemic (left) kidney. In parallel, the UIRI-subjected cKO mice exhibited increased plasma levels of SDMA and ADMA, two early biomarkers of CKD progression[28,33]. SDMA is a dimethylated form of arginine, which is released into the circulation upon protein degradation. It is thought that this molecule indirectly inhibits the nitric oxide synthase (NOS) by decreasing L-arginine availability in endothelial cells. ADMA has been reports to directly inhibit NOS isoforms[34]. It has been shown that ADMA accumulates in IR injured kidneys[35] and that plasma ADMA is a strong prognostic indicator of CKD. Importantly, cKO mice exhibited significantly impaired mitochondrial function in the ischemic kidney compared to kidneys from sham-operated mice and to UIRI-subjected controls. It is well established that mitochondria play a central role in IR-induced kidney damage[36]. A possible explanation for the worsening of mitochondrial function in the ischemic kidney of cKO mice may be provided by the metabolic role of ARG2-generated ornithine in the proximal tubule. Indeed, it has been shown that ARG2 in the kidney co-localizes with ornithine aminotransferase (OAT), an enzyme catalyzing the

conversion of L-ornithine to L-glutamate[11]. L-glutamate, in turn, can be further deaminated to α-ketoglutarate before entering the TCA cycle. Levillain et al. have shown on microdissected tubules that the medullary proximal tubule is the major renal site of CO_2 production from L-ornithine[11]. On the other hand, Weinberg and colleagues have demonstrated that α-ketoglutarate can improve the energy deficit in IR-induced injury by serving as a substrate in an anaerobic pathway of ATP synthesis in the proximal tubule[12]. Thus, it is plausible to hypothesize that stress-induced mitochondrial ARG2 improves cell survival through improvement of both aerobic and anaerobic mitochondrial functions. Evaluating this hypothesis would require new solutions for measurement of metabolic fluxes specifically in the S3 segment.

Collectively, our study demonstrates that ARG2 attenuates kidney damage induced by ischemia-reperfusion injury. Interestingly, other studies performed in *Arg2*-null mice and/or that used nonselective inhibitors of ARG1 and ARG2 suggested a deleterious role of this enzyme in different models of kidney disease, including diabetic nephropathy[15] and high fat diet-induced CKD[37]. While this difference could be due to different types of kidney injury, it could also indicate that the role of ARG2 in kidney stress can be masked by ARG2 and/or ARG1 activity in extra-renal tissues.

MATERIALS AND METHODS

Study approval All experiments with animals were performed in accordance with the Swiss guidelines for animal care (authorisation #29111 (to D.F.)), which conform to the National Institutes of Health animal care guidelines.

Mouse model The *loxP* flanked *Arg2* mice on C57BL/6J background were purchased from Cyagen Biosciences. Animals were maintained ad libitum on the standard laboratory chow diet (KLIBA NAFAG diet 3800). Excision of exons 3, 4, 5 and 6 of the *Arg2* gene was performed with 2 weeks of DOX treatment (2mg DOX + 2g sucrose in 2ml drinking water) of 8-weeks old $Arg2^{lox/lox}$/Pax8-rtTa/LC1 mice (See Results and Supplementary Methods). All experiments were performed on male mice.

Unilateral ischemia-reperfusion injury (UIRI) One month after the end of DOX treatment, mice were anesthetized by intraperitoneal injection of Ketamine:Xylazine (1:1) and shaved on their left side. During the surgical procedure described below, mice were kept on a heated surgical pad maintained at 37°C. An incision of about 15 mm was made on the left side, right below the last rib. Then, the left kidney removed from the peritoneal space. The kidney was maintained out of the peritoneal space with gentle pressure of forceps. Once isolated, both renal artery and vein were clamped (clip vessel 60g, World Precision Instruments) for 25 minutes. During the 25 minutes of clamping, the kidney was replaced back in the peritoneal space and kept hydrated with warm NaCl 0.9% solution. The mice were placed in an environment heated at 37°C (heated box) and the temperature of the ambient air in the box constantly verified using a thermometer to ensure a constant temperature of 37°C during the time of the ischemia. After the 25 minutes of clamping, the clamp was carefully removed and the muscle sutured. In order to avoid reopening of the wound by scratching, the skin was closed using surgical staples. The

wound was disinfected with povidone-iodine and the mice placed under a heat lamp for 12 hours. After 24 hours or 2 weeks of reperfusion, mice were sacrificed. Mice of the sham group were subjected to the same surgery, without clamping and were sacrificed 24 hours or 2 weeks after the surgery.

Protein extraction and Western blot Half kidney was homogenized in RIPA buffer pH8 (20mM Tris, 150mM NaCl, 1% Triton X-100, 0.1% SDS, 0.5% deoxycholate) using a polytron. The homogenate was centrifuged at 4°C and 10,000 x g for 10 minutes and the supernatant sonicated. Protein content in the supernatant was quantified with a Pierce BCA Protein Assay kit (ThermoFisher) and 50µg of protein was mixed with 5X Sample Buffer (bromophenol blue 0.25%, dithiothreitol 0.5 M, 50% glycerol, 10% SDS, Tris-HCl 0.25 M, pH6.8). 12µl of protein sample was loaded on 4%-12% SDS-PAGE gradient gel, run and transferred on nitrocellulose membrane (100V, 2 hours, 4°C). The membrane was then washed with Wash Buffer (TBS-tween 1%), blocked in 2% milk during 1 hour and incubated with the primary antibody (anti-Arg2, Santa Cruz, 1:2,000) at 4°C overnight. The membrane was finally washed a few times with Wash Buffer, incubated with the HRP-coupled secondary antibody (Pierce, 1:5,000) over 1 hour at room temperature and visualized with autoradiography film (Carestream BioMax XAR Film).

RNA extraction and cDNA synthesis Half kidney was homogenized in 2ml of TRI reagent (Sigma) with polytron and the homogenate centrifuged at 4°C and 12,000 x g for 10 minutes to pellet the cellular debris. 200µl of 1-bromo-3-chloropropane (BCP) was added to the supernatant and incubated for 10 minutes at room temperature. After centrifugation, aqueous phase was harvested and RNA precipitated with 1ml of isopropanol. RNA was pelleted by centrifugation (4°C, 12,000 x g, 10 minutes), washed with 75% ethanol and resuspended in

200µl of RNase-free water. cDNA synthesis was performed using PrimeScript RT reagent kit (Takara), according to the manufacturer's instructions. 1µg of RNA was used for retrotranscription.

Quantitative PCR (qPCR) Quantitative PCR were performed with Taqman probes (Applied Biosystems) as follow: Arg2 exons 1-2, ref. Mm1307447_m1; ref. Mm1307452_m1; Vimentin, ref. Mm01333430_m1; Fibronectin, ref. Mm01256744_m1; Col3a1, ref. Mm00802300_m1; Col1a1, ref. Mm00801666_g1. Each qPCR reaction was normalized by GAPDH level (ref. Mm99999915_g1).

Arginase activity Arginase activity was assessed as previously described[38]. Briefly, half kidney was homogenized in 1ml of Lysis Buffer (50mM Tris-HCl pH7.5, 0.1mM EDTA pH8). 5µl of lysate was added to 45µl of Reaction Mix (25µl CHES pH9, 0.5µl $MnCl_2$, 5µl L-Arginine-HCl, 0.5µl ^{14}C-Arginine, 14µl H_2O) and incubated for 60 minutes at 37°C to allow urea formation. The reaction was then stopped by adding 200µl of Stop Solution, pH4.5 (7M Urea, 10mM L-Arginine, 0.25M Acetic acid) with 100µl of H_2O and 100mg of Dowex. Samples were finally centrifuged (10 minutes at 6,000 x g) and 50µl of supernatant was taken for radioactivity counting.

Immunohistochemistry Kidneys were fixed by intrarenal perfusion of 2% PFA, paraffin-embedded, cut into 3 µm sections using a microtome and mounted on Superfrost Plus Slides. Prior to start the immunohistochemistry experiment, slides were deparaffinized by successive immersion into baths of xylol (twice), 100% ethanol (twice), 95% ethanol, 80% ethanol and finally rinsed with tap water. Slides were then treated with Antigen Retrieval Buffer (10mM Na-citrate, 1mM EDTA), boiled in a microwave over for 15 minutes, and blocked with

Blocking Solution (10% normal goat serum, 0.05% Tween, 1X PBS, 4 drops of Avidin block from Avidin/Biotin Blocking Kit (Vector)) for 1 hour at room temperature. Sections were washed a few times with 1X PBS and then overnight incubated with primary antibody (anti-Arg2, Santa Cruz, 1:1000 in Blocking Solution and Biotin (from Avidin/Biotin Blocking Kit (Vector)) at 4°C. The day after, slides were washed few times with 1X PBS, incubated with 0.3% H_2O_2 for 30 minutes at room temperature to block the endogenous peroxidase and finally with the secondary biotinylated-antibody (1:200, Vector) for 30 minutes at room temperature. Following a few washings with 1X PBS, sections were treated for 30 minutes at room temperature with ABC reagent (Vectastain ABC Kit Elite, Vector) and signal was revealed with NovaRED (Vector). Slides were finally dehydrated by successive immersions in 70% ethanol, 90% ethanol and 100% ethanol (twice). Slides were mounted with hydrophobic media Röti Histokit and stored at room temperature until image acquisition.

Scoring of tubular injury Kidney sections were Periodic acid-Schiff (PAS)-stained and tubular injury was blindly assessed by 3 independent pathologists who examined 9 different slides for each genotype. A score was attributed to each slide, according to the level of injury and following the scoring system as described: 0 = no damage; 1 = < 35% injured tubules; 2 = 25% - 49% injured tubules; 3 = 50% - 75% injured tubules and 4 = > 75% injured tubules.

TUNEL assay TUNEL staining was performed using an In Situ Cell Death Detection Kit, (Roche). Left kidneys of 6 Control and 6 cKO mice were fixed by intrarenal perfusion of 2% PFA, paraffin-embedded, cut in 3µm longitudinal sections using a microtome and mounted on Superfrost Plus Slides. Staining of kidney sections was performed according to manufacturer instructions. After staining, slides were scanned using Zeiss Axioscan Z1 and stained area quantified by QuPath software.

Corticomedullary urea and osmolality gradient Kidneys were harvested from mice sacrificed by cervical dislocation. On ice, cortex, outer medulla and inner medulla were separated, placed in 1.5 ml Eppendorf tubes and dried for 12 hours at 60°C. The dried tissue was then weighed and 15, 25 and 35 volumes of ddH_2O were added to 1 mg of dried cortex, outer medulla and inner medulla, respectively, before being heated at 90°C for 3 minutes and overnight stored at 4°C. The next day, tubes were centrifuged and supernatants recovered for analysis. Urea content was determined by the Laboratoire Central de Chimie Clinique (LCC) of the Centre Hospitalier Universitaire Vaudois (CHUV) (Lausanne, Switzerland) while osmolality was assessed using freezing point depression (Osmometer 2020, Advances Instruments).

Plasma and urine chemistry Urinary and plasma Na^+ and K^+ concentrations were measured by flame photometry (Instrumentation Laboratory 943). Osmolality was determined using freezing point depression (Osmometer 2020, Advances Instruments) and urinary pH assessed with a pH meter (Metrohm). Urinary Ca^{2+}, Mg^{2+}, phosphate, creatinine, glucose, urate and albumin concentrations as well as plasma and urinary concentrations of urea were measured by the LCC of the CHUV. Urinary amino acids and plasma concentrations of arginine, citrulline, ornithine, ADMA, SDMA and creatinine were measured by Biocrates Life Sciences (Innsbruck, Austria).

Mitochondrial isolation Medullas of right and left kidneys after 2 weeks of reperfusion following renal ischemia were homogenized in 2ml cold isolation buffer (10mM Tris, 200mM sucrose, 1mM EGTA/Tris, protease inhibitor cocktail pH to 7.4). Tissue homogenization was obtained after 20 strokes at 1500rpm. Two rounds of centrifugation at 800g for 10 min at 4°C were performed in order to remove cellular debris. The mitochondrial fraction was pelleted at

10000g for 10 min at 4°C and subsequently washed using isolation buffer. The mitochondrial pellet was suspended in 200ul isolation buffer and quantified with a Pierce BCA Protein Assay kit (Thermofisher). Mitochondria were immediately used for Seahorse analysis.

Seahorse Analyses Mitochondrial function was determined with an XFe-24 extracellular flux analyzer (Seahorse Bioscience). Oxygen consumption rate (OCR) was assessed using 50µl of mitochondrial suspension (5µg of freshly isolated mitochondria) per well. The V7-PS cell culture plate was centrifuged at 2000g for 20 min at 4°C and 475µl of MAS 1X assay medium (70mM sucrose, 220mM mannitol, 10mM KH_2PO_4, 5mM MgCl2, 2mM Hepes, 10mM EGTA, 0.2% fatty acid-free BSA, pH7.2) containing 10mM succinate (Sigma-Aldrich) and 2µM Rotenone (Sigma-Aldrich) was added into each well. After 10 min of incubation at 37°C without CO_2, mitochondrial respiration was measured followed by successive injections of 5mM ADP (Sigma-Aldrich), 1µM Oligomycin (Sigma-Aldrich), 4µM of carbonylcyanide p-trifluoromethoxyphenylhydrazone (FCCP) (Sigma-Aldrich) and 4µM antimycin A (Sigma-Aldrich). All respiration results were normalized by mitochondrial protein content.

Polyamines levels in kidney tissue Kidney tissue levels of putrescine, spermidine and spermine were determined by Metabolon® (Potsdam, Germany) using UPLC-MS/MS.

GFR GFR was measured on anesthetized animals with inulin-FITC as previously described[39]. Briefly, ~2.5% FITC-inulin (2 µl/g BW) was injected into the retro-orbital plexus of Control or cKO mice. Blood collection was performed 3, 7, 10, 15, 40 and 60 minutes post-injection. Inulin clearance was calculated using a two phase exponential decay curve model[40].

Statistics All data are expressed as mean ± SEM. Normality of distribution has been tested using Shapiro-Wilk test to ensure that data meet the requirements for parametric tests. Alternative nonparametric tests have been used when necessary. Statistical tests are described in Figure legends. $p < 0.05$ was considered significant.

AUTHORS CONTRIBUTION

CA, HAIY, SR, FA and DF designed experiments and interpreted results. CA, GC and SL carried out most of the experimental work with the help of SN, MM, JLB and ND. SP performed all statistical analyses. CA, SL, FA and DF analyzed the data and wrote the manuscript.

ACKNOWLEDGMENTS This work was supported by Swiss National Science Foundation Research Grant 31003A-169493 (to D.F.) and by the Russian Federal Agency of Scientific Organizations Grant AAAA-A18-118012290371-3 (to S.N.). Selected data in this manuscript were previously presented at the Experimental Biology 2018 meeting. The authors thank Drs. Lise Bankir and Olivier Bonny for their helpful discussions.

CONFLICT OF INTERESTS

None

1. Ochocki JD, Khare S, Hess M, et al. Arginase 2 Suppresses Renal Carcinoma Progression via Biosynthetic Cofactor Pyridoxal Phosphate Depletion and Increased Polyamine Toxicity. *Cell metabolism.* 2018;27(6):1263-1280.e1266.
2. Zaytouni T, Tsai PY, Hitchcock DS, et al. Critical role for arginase 2 in obesity-associated pancreatic cancer. *Nature communications.* 2017;8(1):242.
3. Xu W, Ghosh S, Comhair SA, et al. Increased mitochondrial arginine metabolism supports bioenergetics in asthma. *J Clin Invest.* 2016;126(7):2465-2481.
4. Ryoo S, Gupta G, Benjo A, et al. Endothelial arginase II: a novel target for the treatment of atherosclerosis. *Circ Res.* 2008;102(8):923-932.
5. Zhang Y, Higgins CB, Fortune HM, et al. Hepatic arginase 2 (Arg2) is sufficient to convey the therapeutic metabolic effects of fasting. *Nature communications.* 2019;10(1):1587.
6. Suwanpradid J, Rojas M, Behzadian MA, Caldwell RW, Caldwell RB. Arginase 2 deficiency prevents oxidative stress and limits hyperoxia-induced retinal vascular degeneration. *PLoS One.* 2014;9(11):e110604.
7. Caldwell RW, Rodriguez PC, Toque HA, Narayanan SP, Caldwell RB. Arginase: A Multifaceted Enzyme Important in Health and Disease. *Physiol Rev.* 2018;98(2):641-665.
8. Levillain O, Hus-Citharel A, Morel F, Bankir L. Localization of arginine synthesis along rat nephron. *Am J Physiol.* 1990;259(6 Pt 2):F916-923.
9. Levillain O, Hus-Citharel A, Morel F, Bankir L. Production of urea from arginine in pars recta and collecting duct of the rat kidney. *Renal physiology and biochemistry.* 1989;12(5-6):302-312.
10. Levillain O, Hus-Citharel A, Morel F, Bankir L. Localization of urea and ornithine production along mouse and rabbit nephrons: functional significance. *Am J Physiol.* 1992;263(5 Pt 2):F878-885.
11. Levillain O, Hus-Citharel A, Garvi S, et al. Ornithine metabolism in male and female rat kidney: mitochondrial expression of ornithine aminotransferase and arginase II. *Am J Physiol Renal Physiol.* 2004;286(4):F727-738.
12. Weinberg JM, Venkatachalam MA, Roeser NF, et al. Anaerobic and aerobic pathways for salvage of proximal tubules from hypoxia-induced mitochondrial injury. *Am J Physiol Renal Physiol.* 2000;279(5):F927-943.
13. Weinberg JM, Venkatachalam MA, Roeser NF, Nissim I. Mitochondrial dysfunction during hypoxia/reoxygenation and its correction by anaerobic metabolism of citric acid cycle intermediates. *Proc Natl Acad Sci U S A.* 2000;97(6):2826-2831.
14. Raup-Konsavage WM, Gao T, Cooper TK, Morris SM, Jr., Reeves WB, Awad AS. Arginase-2 mediates renal ischemia-reperfusion injury. *Am J Physiol Renal Physiol.* 2017;313(2):F522-f534.
15. Morris SM, Jr., Gao T, Cooper TK, Kepka-Lenhart D, Awad AS. Arginase-2 mediates diabetic renal injury. *Diabetes.* 2011;60(11):3015-3022.
16. Romero MJ, Yao L, Sridhar S, et al. l-Citrulline Protects from Kidney Damage in Type 1 Diabetic Mice. *Frontiers in immunology.* 2013;4:480.
17. Akomolafe SF, Akinyemi AJ, Anadozie SO. Phenolic Acids (Gallic and Tannic Acids) Modulate Antioxidant Status and Cisplatin Induced Nephrotoxicity in Rats. *International scholarly research notices.* 2014;2014:984709.
18. Lacroix C, Caubet C, Gonzalez-de-Peredo A, et al. Label-free quantitative urinary proteomics identifies the arginase pathway as a new player in congenital obstructive nephropathy. *Mol Cell Proteomics.* 2014;13(12):3421-3434.

19. Levillain O. Expression and function of arginine-producing and consuming-enzymes in the kidney. *Amino Acids.* 2012;42(4):1237-1252.
20. Huang J, Montani JP, Verrey F, Feraille E, Ming XF, Yang Z. Arginase-II negatively regulates renal aquaporin-2 and water reabsorption. *Faseb j.* 2018;32(10):5520-5531.
21. Nikolaeva S, Ansermet C, Centeno G, et al. Nephron-Specific Deletion of Circadian Clock Gene Bmal1 Alters the Plasma and Renal Metabolome and Impairs Drug Disposition. *J Am Soc Nephrol.* 2016;27(10):2997-3004.
22. Traykova-Brauch M, Schonig K, Greiner O, et al. An efficient and versatile system for acute and chronic modulation of renal tubular function in transgenic mice. *Nat Med.* 2008;14(9):979-984.
23. Sorensen-Zender I, Rong S, Susnik N, et al. Role of fibrinogen in acute ischemic kidney injury. *Am J Physiol Renal Physiol.* 2013;305(5):F777-785.
24. Liu J, Kumar S, Dolzhenko E, et al. Molecular characterization of the transition from acute to chronic kidney injury following ischemia/reperfusion. *JCI insight.* 2017;2(18).
25. Le Clef N, Verhulst A, D'Haese PC, Vervaet BA. Unilateral Renal Ischemia-Reperfusion as a Robust Model for Acute to Chronic Kidney Injury in Mice. *PLoS One.* 2016;11(3):e0152153.
26. Montgomery TA, Xu L, Mason S, et al. Breast Regression Protein-39/Chitinase 3-Like 1 Promotes Renal Fibrosis after Kidney Injury via Activation of Myofibroblasts. *J Am Soc Nephrol.* 2017;28(11):3218-3226.
27. Tain YL, Hsu CN. Toxic Dimethylarginines: Asymmetric Dimethylarginine (ADMA) and Symmetric Dimethylarginine (SDMA). *Toxins.* 2017;9(3).
28. Emrich IE, Zawada AM, Martens-Lobenhoffer J, et al. Symmetric dimethylarginine (SDMA) outperforms asymmetric dimethylarginine (ADMA) and other methylarginines as predictor of renal and cardiovascular outcome in non-dialysis chronic kidney disease. *Clinical research in cardiology : official journal of the German Cardiac Society.* 2018;107(3):201-213.
29. Kochakian CD. The effect of dose and nutritive state on kidney arginase after steroid stimulation. *J Biol Chem.* 1945;161:115-125.
30. Dounce AL, Beyer GT. The arginase activity of isolated cell nuclei. *J Biol Chem.* 1948;174(3):859-872.
31. Brezis M, Agmon Y, Epstein FH. Determinants of intrarenal oxygenation. I. Effects of diuretics. *Am J Physiol.* 1994;267(6 Pt 2):F1059-1062.
32. Hall AM, Unwin RJ. The not so 'mighty chondrion': emergence of renal diseases due to mitochondrial dysfunction. *Nephron Physiol.* 2007;105(1):p1-10.
33. Betz B, Moller-Ehrlich K, Kress T, et al. Increased symmetrical dimethylarginine in ischemic acute kidney injury as a causative factor of renal L-arginine deficiency. *Translational research : the journal of laboratory and clinical medicine.* 2013;162(2):67-76.
34. Teerlink T, Luo Z, Palm F, Wilcox CS. Cellular ADMA: regulation and action. *Pharmacological research.* 2009;60(6):448-460.
35. Nakayama Y, Ueda S, Yamagishi S, et al. Asymmetric dimethylarginine accumulates in the kidney during ischemia/reperfusion injury. *Kidney Int.* 2014;85(3):570-578.
36. Hall AM, Schuh CD. Mitochondria as therapeutic targets in acute kidney injury. *Curr Opin Nephrol Hypertens.* 2016;25(4):355-362.

37. Huang J, Rajapakse A, Xiong Y, et al. Genetic Targeting of Arginase-II in Mouse Prevents Renal Oxidative Stress and Inflammation in Diet-Induced Obesity. *Frontiers in physiology.* 2016;7:560.
38. Kepka-Lenhart D, Ash DE, Morris SM. Determination of mammalian arginase activity. *Methods Enzymol.* 2008;440:221-230.
39. Eisner C, Faulhaber-Walter R, Wang Y, et al. Major contribution of tubular secretion to creatinine clearance in mice. *Kidney Int.* 2010;77(6):519-526.
40. Qi Z, Whitt I, Mehta A, et al. Serial determination of glomerular filtration rate in conscious mice using FITC-inulin clearance. *Am J Physiol Renal Physiol.* 2004;286(3):F590-596.

Table 1. Urine and plasma chemistry of sham-operated Control and cKO mice and, of Control and cKO mice subjected to 25 minutes unilateral renal ischemia followed by 24 hours of reperfusion.

							Sham vs UIRI 24h	
	Sham			UIRI 24h			*Control*	*cKO*
	Control (n=5)	cKO (n=5)	*p*	Control (n=5)	cKO (n=5)	*p*	*p*	*p*
24-hour urine								
Volume/g BW (ml/g BW)	0.013 ± 0.002	0.012 ± 0.002	*NS*	0.023 ± 0.004	0.047 ± 0.065	*<0.01*	*NS*	*<0.01*
Osmolality (mOsm/kg H_2O)	3100 ± 393	3423 ± 418	*NS*	1943 ± 240	1568 ± 162	*NS*	*0.056*	*<0.01*
pH	5.50 ± 0.06	5.57 ± 0.05	*NS*	5.69 ± 0.12	5.71 ± 0.04	*NS*	*NS*	*NS*
UV x Na^+/ g BW (µmol/g)	1.41 ± 0.36	0.62 ± 0.22	*NS*	1.55 ± 0.47	1.66 ± 0.33	*NS*	*NS*	*NS*
UV x K^+/g BW (µmol/g)	4.00 ± 0.49	3.26 ± 0.43	*NS*	4.57 ± 0.84	7.57 ± 0.83	*0.02*	*NS*	*<0.01*
UV x Ca^{2+}/g BW (µmol/g)	0.021 ± 0.007	0.012 ± 0.002	*NS*	0.033 ± 0.006	0.067 ± 0.009	*<0.01*	*NS*	*<0.001*
UV x Mg^{2+}/g BW (µmol/g)	0.63 ± 0.08	0.72 ± 0.12	*NS*	1.01 ± 0.20	1.73 ± 0.15	*0.01*	*NS*	*<0.01*
UV x PO_4^{3-}/g BW (µmol/g)	2.25 ± 0.11	2.24 ± 0.21	*NS*	2.69 ± 0.61	4.63 ± 0.63	*NS*	*NS*	*0.014*
UV x Creatinine/g BW (µmol/g)	0.10 ± 0.01	0.09 ± 0.01	*NS*	0.09 ± 0.02	0.14 ± 0.01	*NS*	*NS*	0.07
UV x Urea/g BW (µmol/g)	21.8 ± 2.8	24.1 ± 3.2	*NS*	23.3 ± 5.4	40.9 ± 3.2	*0.02*	*NS*	0.06
UV x Glucose/g BW (µmol/g)	0.54 ± 0.42	0.82 ± 0.35	*NS*	2.39 ± 0.62	1.75 ± 0.37	*NS*	*0.06*	*NS*
UV x Urate /g BW (µmol/g)	0.022 ± 0.005	0.022 ± 0.003	*NS*	0.009 ± 0.002	0.009 ± 0.002	*NS*	*NS*	*NS*
UV x Albumin (µg/g BW)	0.29 ± 0.05	0.29 ± 0.07	*NS*	0.93 ± 0.33	2.08 ± 0.34	*0.04*	*NS*	*<0.01*
UV* Ornithine (nmol/g BW)	0.03 ± 0.01	0.02 ± 0.01	*NS*	0.22 ± 0.06	2.66 ± 2.11	*NS*	*NS*	*NS*
UV*Citrulline (nmol/g BW)	0.20 ± 0.04	0.33 ± 0.10	*NS*	1.78 ± 0.46	4.71 ± 1.18	*0.022*	*NS*	*<0.01*
Plasma								
Na^+ (mM)	155 ± 3.7	151 ± 0.5	*NS*	151.0 ± 0.9	151.8 ± 0.7	*NS*	*NS*	*NS*
K^+ (mM)	4.25 ± 0.17	4.14 ± 0.20	*NS*	3.55 ± 0.13	3.78 ± 0.16	*NS*	*0.04*	*NS*
Urea (mM)	6.45 ± 0.80	5.84 ± 0.53	*NS*	8.33 ± 0.55	6.48 ± 0.22	*0.04*	*0.03*	*NS*
Arginine (µM)	104.1 ± 8.9	114.8 ± 12.4	*NS*	95.3 ± 11.2	114.8 ± 16.7	*NS*	*NS*	*NS*
Citrulline (µM)	56.1 ± 3.3	55.4 ±5.9	*NS*	50.9 ± 4.4	49.3 ± 4.3	*NS*	*NS*	*NS*
Ornithine (µM)	56.1 ± 3.7	69.1 ± 13.5	*NS*	84.4 ± 1.6	89.6 ± 8.8	*NS*	*0.08*	*NS*
ADMA (µM)	0.67 ± 0.04	0.77 ± 0.05	*NS*	0.81 ± 0.03	0.90 ± 0.03	*NS*	*0.08*	*NS*
SDMA (µM)	0.21 ± 0.01	0.21 ± 0.01	*NS*	0.26 ± 0.01	0.29 ± 0.01	*NS*	*0.04*	*<0.001*
Creatinine (µM)	14.1 ± 3.2	13.6 ± 3.0	*NS*	19.6 ± 1.3	18.1 ± 1.1	*NS*	*NS*	*NS*

Urine samples were collected in metabolic cages over 24 hours following UIRI or sham surgery. Data are mean±SEM. Two-way ANOVA with Tukey's multiple comparisons test.

FIGURE LEGENDS

Figure 1. (A) Relative Arg2 mRNA expression in kidneys of Control and cKO mice (mean±SEM, *n*=7 Control mice, *n*=5 cKO mice, unpaired *t*-test, ***p<0.001). 100% corresponds to the mean of Arg2 mRNA expression in kidney from Control mice. (B) Western blot analysis of ARG2 protein expression in kidneys of Control and cKO mice. The original full-length Western blot images for ARG2 and GAPDH are shown in Supplementary Figure 9A. (C) Arginase activity in kidneys of Control and cKO mice (mean±SEM, *n*=7 Control mice, *n*=5 cKO mice, unpaired *t*-test, ***p<0.001). (D) Relative Arg2 mRNA expression in the liver of Control and cKO mice (mean±SEM, *n*=7 Control mice, *n*=5 cKO mice). 100% corresponds to the mean of Arg2 mRNA expression in kidney from Control mice. (E) Percentage of kidney weight to body weight in Control and cKO mice (mean±SEM, *n*=7 Control mice, *n*=5 cKO mice, unpaired *t*-test, **p<0.01). Details of statistical analysis are presented in Supplementary Statistical Table for Figures 1 to 6.

Figure 2. (A) Relative Arg2 mRNA expression in right (R) and left (L) kidney of Control mice after left kidney ischemia followed by 24 hours of reperfusion (UIRI 24h) or after sham surgery (mean±SEM, *n*=5 for sham-operated Control mice, n=7 for UIRI-operated Control mice, two-way repeated measures ANOVA with Sidak's multiple comparisons test, **p<0.01). 100% corresponds to the mean of Arg2 mRNA expression in the right kidney from sham-operated Control mice. (B) Relative Arg2 mRNA expression in right (R) and left (L) kidney of cKO mice after left kidney ischemia followed by 24 hours of reperfusion (UIRI 24h) or after sham surgery (mean±SEM, *n*=5 for sham-operated Control mice, n=7 for UIRI-operated cKO mice,

two-way repeated measures ANOVA with Sidak's multiple comparisons test, ***p<0.001). 100% corresponds to the mean of Arg2 mRNA expression in the right kidney from sham-operated Control mice. (C) Immunohistochemistry analysis of ARG2 expression and localization in right and left kidneys of Control mice subjected to left kidney ischemia followed by 24 hours of reperfusion. Details of statistical analysis are presented in Supplementary Statistical Table for Figures 1 to 6.

Figure 3. (A-B) Periodic Acid-Schiff (PAS)-stained kidney sections from Control and cKO mice, respectively, after left kidney ischemia followed by 24 hours of reperfusion (C) Scores of damaged tubules in right and left cortex (C.) and medulla (Med.) of Control and cKO mice subjected to left kidney ischemia followed by 24 hours of reperfusion. mean±SEM, *n*=5 for right kidney, *n*=9 for left kidney, Mann-Whitney test, *p<0.05. (D-E) Representative TUNEL (Terminal deoxynucleotidyl transferase dUTP nick end labeling) staining of ischemic left kidney from Control and cKO mice after 24 hours of reperfusion. (F) Percentage of TUNEL-stained area in left ischemic kidney of Control and cKO mice after 24 hours of reperfusion (mean±SEM, *n*=6, unpaired *t*-test). Details of statistical analysis are presented in Supplementary Statistical Table for Figures 1 to 6.

Figure 4. (A) Urea content in cortex, outer and inner medulla in right and left kidney of Control (black circle) and cKO mice (white circle) 24 hours after sham surgery. Mean±SEM, *n*=7 Control mice, *n*=6 cKO mice, unpaired *t*-test and Mann-Whitney test, *p<0.05, **p<0.01. (B) Overall osmolyte content in cortex, outer and inner medulla in right and left kidney of Control (black circle) and cKO mice (white circle) 24 hours after sham surgery. Mean±SEM, *n*=7 for right and left cortex of Control mice, *n*=6 for right and left cortex of cKO mice and for right and left outer medulla of Control and cKO mice, respectively. *n*=5 for right and left outer

medulla of Control and cKO mice, respectively. Unpaired *t*-test, *p<0.05. (C) Urea content in cortex, outer and inner medulla in right and left kidney of Control (black circle) and cKO mice (white circle) 24 hours after left kidney ischemia (UIRI 24h). Mean±SEM, *n*=7 Control mice, *n*=6 cKO mice, **p<0.01, ***p<0.001, Wilcoxon matched-pairs signed rank test, statistical difference between right and left kidney; §p<0.01, §§p<0.01, Mann-Whitney test, statistical difference between urea content measured 24 hours after left kidney ischemia and urea content measured 24 hours after sham surgery (shown in panel A). (D) Overall osmolyte content in cortex, outer and inner medulla in right and left kidney of Control (black circle) and cKO mice (white circle) 24 hours after left kidney ischemia (UIRI 24h). Mean±SEM, *n*=7 for right and left cortex of Control mice, *n*=6 for right and left cortex of cKO mice and for left outer medulla of Control and cKO mice, *n*=5 and *n*=3 for right outer medulla of Control and cKO mice, respectively. Details of statistical analysis are presented in Supplementary Statistical Table for Figures 1 to 6.

Figure 5. (A) Body weight of Control and cKO mice after renal ischemia followed by 14 days of reperfusion (UIRI 14d), *n*=6, unpaired *t*-test, *p<0.05. (B) Relative weights of right and left kidneys after 14 days of reperfusion following renal ischemia. 100% corresponds to the mean of kidney weights from the corresponding sham group (mean±SEM, *n*=10 for UIRI-subjected cKO mice; *n*=7 for UIRI-subjected Control mice, two-way repeated measures ANOVA with Sidak's multiple comparisons test, **p<0.01, ***p<0.001). (C) Immunohistochemistry analysis of ARG2 expression and localization in right and left kidney of Control mice subjected to left kidney ischemia followed by 14 days of reperfusion (UIRI 14d). (D) Correlation between relative expressions of Arg2 and markers of fibrosis in the left kidney of UIRI-subjected Control mice (14 days of reperfusion). 1 corresponds to expression levels of Arg2, Vim, Fn1, Col3a1 and Col1a1 in the right kidney of sham-operated Control mice. R-squared and p-value

for linear regression. (E) Plasma levels of SDMA and ADMA in Control and cKO mice subjected to renal ischemia followed by 14 days of reperfusion (UIRI 14d) or to sham surgery (mean±SEM, n=5 for sham groups, n=10 for UIRI 14d groups, two-way ANOVA with Tukey's multiple comparisons test, *p<0.05, **p<0.01). Details of statistical analysis are presented in Supplementary Statistical Table for Figures 1 to 6.

Figure 6. (A) Oxygen consumption rate (OCR) of isolated mitochondria in right and left kidney of Control and cKO mice after 14 days of reperfusion following left kidney ischemia. (B) Basal respiration (state II) of mitochondrial complex II (using succinate as substrate) while inhibiting complex I (Rotenone). (C) ADP-stimulated respiration (state III) following an acute injection of ADP. (D) Resting respiration (state IVo) following the acute inhibition of complex V (oligomycin). (E) Maximal uncoupled respiration (state IIIu) following an acute injection of carbonyl cyanide p-trifluoro-methoxyphenyl hydrazine (FCCP). Mean±SEM, *n*=3 UIRI-subjected Control and cKO mice. For each mouse at least 4 technical replicates were performed. Two-way repeated measures ANOVA. Details of statistical analysis are presented in Supplementary Statistical Table for Figures 1 to 6.

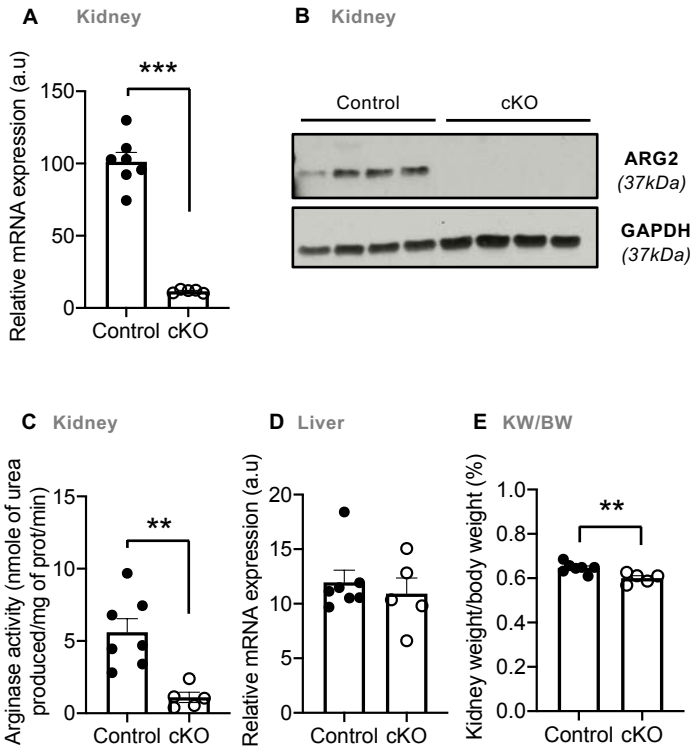

Figure 1. Ansermet et al.

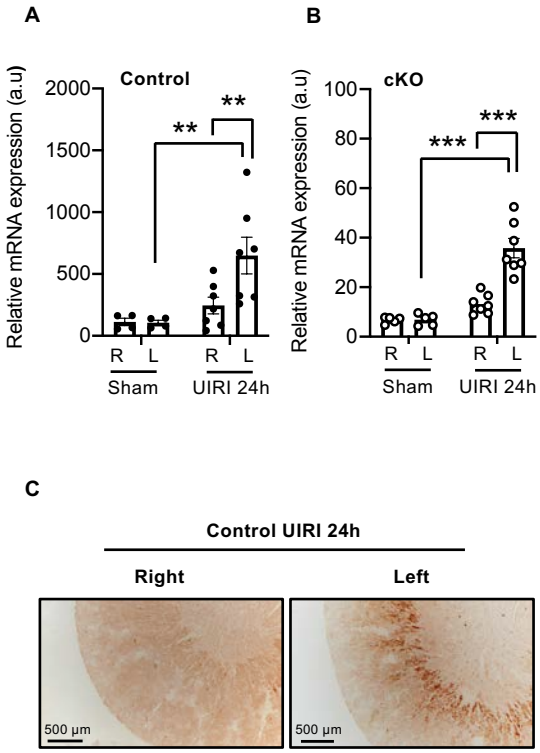

Figure 2. Ansermet et al.

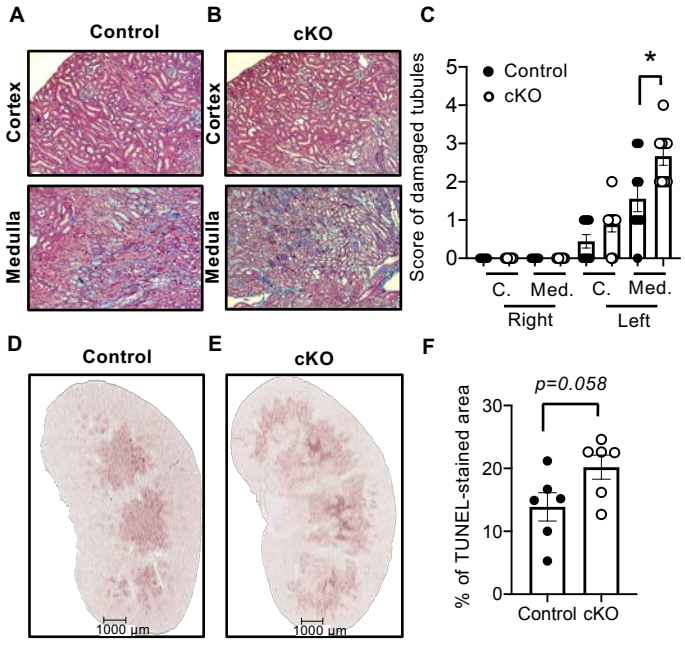

Figure 3. Ansermet et al.

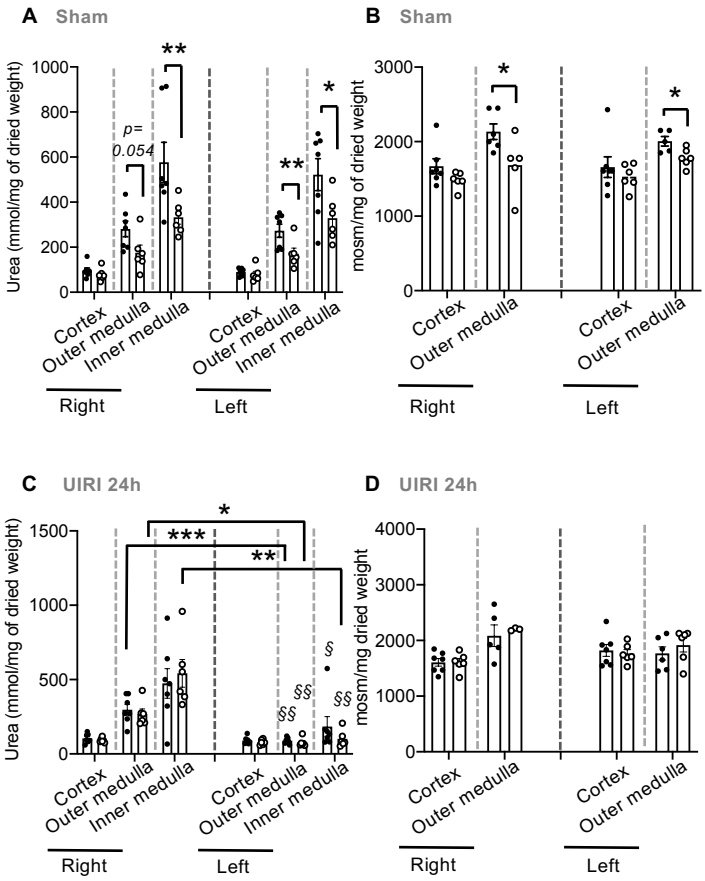

Figure 4. Ansermet et al.

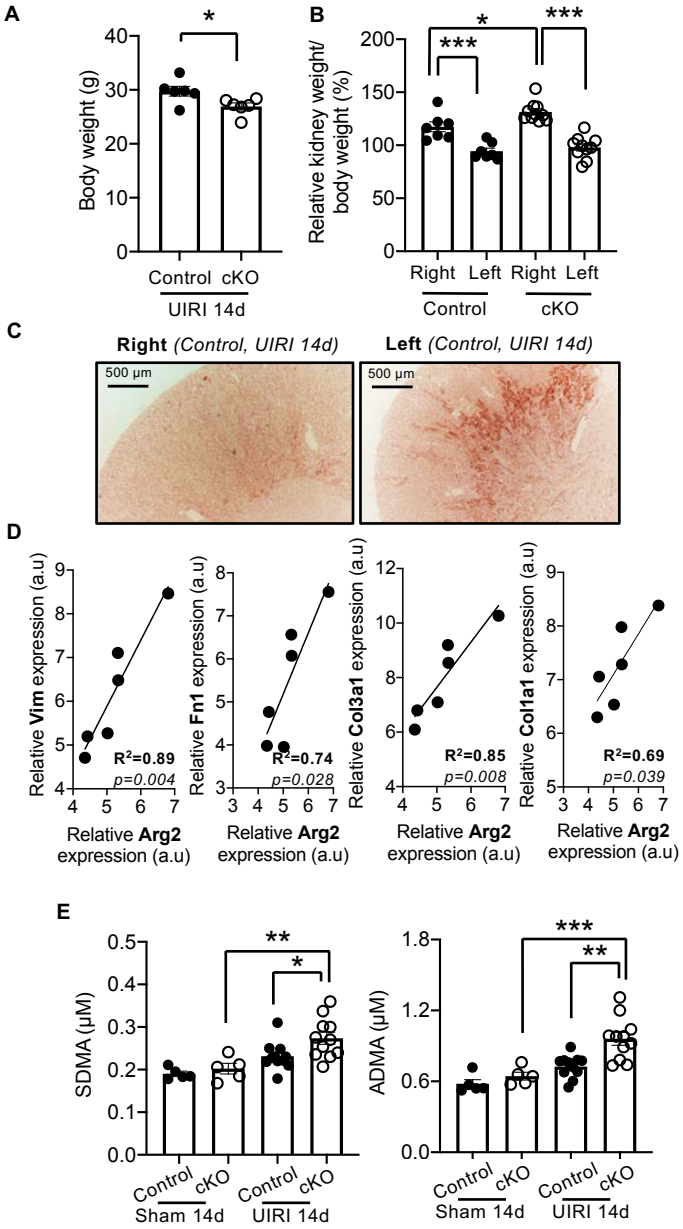

Figure 5. Ansermet et al.

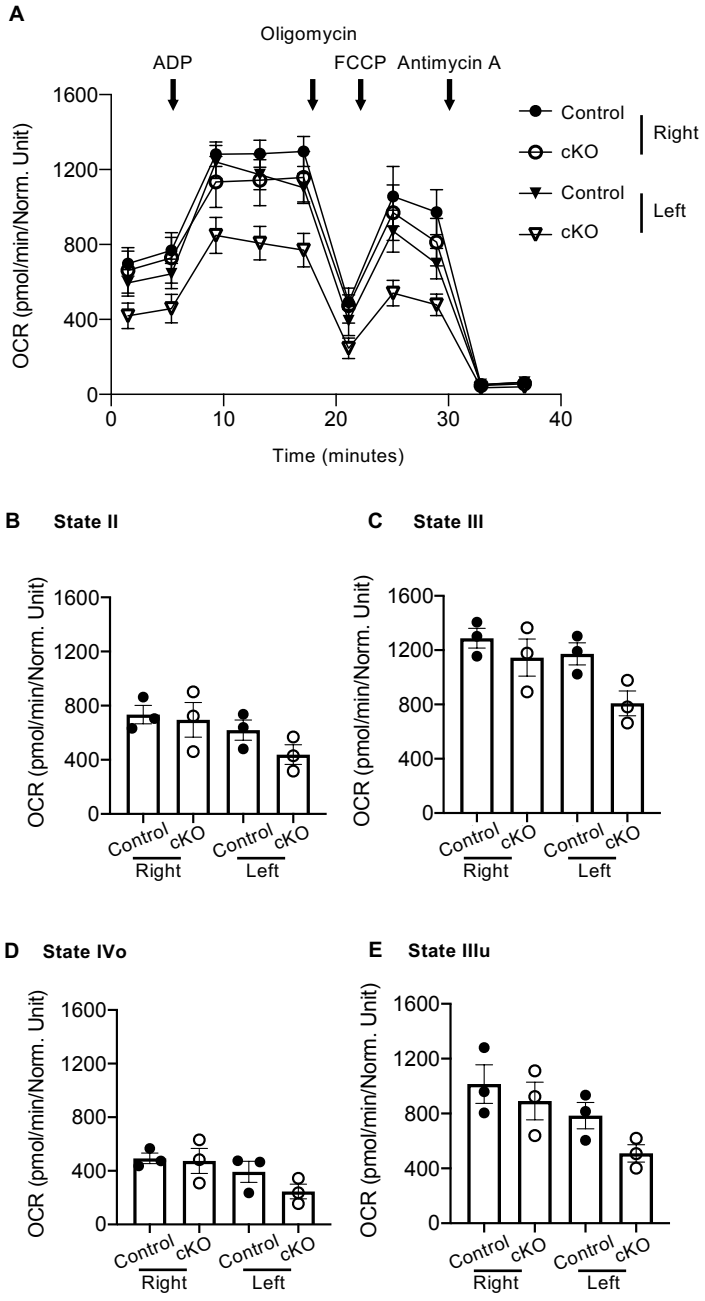

Figure 6. Ansermet et al.